IBRACON Structures and Materials Journal
Revista IBRACON de Estruturas e Materiais
ISSN 1983-4195 ismj.org

ORIGINAL ARTICLE

Characterization of self-compacting concrete incorporating fly ash and rice husk ash at fresh and hardened state

Caracterização de concreto autoadensável no estado fresco e endurecido incorporando cinza volante e cinza de casca de arroz

Luis Eduardo Kosteski[a]
Ederli Marangon[a]
Jarbas Bressa Dalcin[a]
Matheus Machado Costa[a]

[a]Universidade Federal do Pampa – UNIPAMPA, Alegrete, RS, Brasil

Received 8 March 2024
Revised 2 July 2024
Accepted 22 July 2024

Abstract: This work studies the feasibility of using rice husk ash (RHA) as a partial replacement for Brazilian Portland cement in producing self-compacting concrete for structural purposes. The RHA used is produced under controlled burning conditions in a fluidized bed. The concrete mix design is presented in detail to show how to find the best combination of the regional material to produce self-compacting concretes with good fresh and hardened characteristics. Concretes produced in the proportions of 5%, 10%, 15%, 20%, and 25% of replacement of cement by RHA have been studied, with the addition of 15% of fly ash and w/b of 0.45. In the fresh state, flowability, viscosity, and passing ability tests have been conducted. Additionally, mechanical tests were performed to assess the axial compressive strength and splitting tensile strength in the hardened state. The fresh state properties are influenced by the RHA content, reducing its flowability and passing ability with the increase of this material. The hardened state properties of the mixtures with RHA have shown increased resistance when compared to plain concrete. The mixture with 15% replacement had the best results. Concretes of 20% and 25% had their strength increased to a lesser degree. However, they remain a good option when increasing the superplasticizer quantity to improve the fluid state's properties.

Keywords: self-compacting concrete, rice husk ash, fly ash, fresh properties, hardened properties, concrete mix design.

Resumo: Este trabalho estuda a viabilidade da utilização da cinza de casca de arroz (CCA) como substituto parcial do cimento Portland brasileiro na produção de concreto autoadensável para fins estruturais. O CCA utilizado é produzido em condições controladas de queima em um leito fluidizado. O projeto da mistura de concreto é apresentado detalhadamente para mostrar como encontrar a melhor combinação do material regional para produzir concretos autoadensáveis com boas características nas condições frescas e endurecidas. Concretos produzidos nas proporções de 5%, 10%, 15%, 20% e 25% de substituição do cimento por CCA foram estudados, com adição de 15% de cinza volante e relação a/b de 0.45. No estado fresco, realizaram-se testes de fluidez, viscosidade e habilidade passante. Além disso, testes mecânicos foram realizados para avaliar as resistências à compressão axial e à tração por compressão diametral no estado endurecido. As propriedades no estado fresco são influenciadas pela quantidade de CCA, reduzindo sua fluidez e capacidade de passagem com o aumento deste material. As propriedades no estado endurecido das misturas com CCA demonstraram maior resistência em comparação com o concreto simples. A mistura com 15% de substituição apresentou os melhores resultados. Os concretos com 20% e 25% apresentaram menor aumento de resistência. Entretanto, permanecem como uma boa opção ao aumentar a quantidade de superplastificante para melhorar as propriedades no estado fluido.

Palavras-chave: concreto autoadensável, cinza de casca de arroz, cinza volante, propriedades no estado fresco, propriedades no estado endurecido, design de mistura de concreto.

Corresponding author: Luis Eduardo Kosteski. E-mail: luiskosteski@unipampa.edu.br
Financial support: None.
Conflict of interest: Nothing to declare.
Data Availability: The data that support the findings of this study are available from the corresponding author, LEK, upon reasonable request.

How to cite: L. E. Kosteski, E. Marangon, J. B. Dalcin, and M. M. Costa, "Characterization of self-compacting concrete incorporating fly ash and rice husk ash at fresh and hardened state," *Rev. IBRACON Estrut. Mater.*, vol. 17, no. 2, e17215, 2024, https://doi.org/10.1590/S1983-41952024000200015

1 INTRODUCTION

Over half of the world's population relies on rice as its primary food source. In Brazil, annual rice production exceeds 10 million tons, with the state of Rio Grande do Sul accounting for over 70% of this output [1]. The residue from rice production is considerable, mainly comprising broken rice, rice bran, rice straw, and husks. However, the food industry can fully utilize the broken rice and rice bran (sold to manufacture animal food, for example) [2]. The rice straw can be used to produce fuel and various other products, as has shown by Abraham et al. [3]. In order to have a production cycle with zero waste, the rise husk and straw can be used to manufacture light materials for increased acoustic and thermal insulation [4], [5]. It is worth noting that the rice husks, which represent about 20-25% of the grain weight, are a material with a high calorific value, making it a great source of biomass [6], [7]. Generally, rice husk ashes (RHA) are released into the environment after being burnt during biomass production. When the burning process is performed under temperature and time-controlled conditions, RHA may be retrieved and used as a raw material by the construction industry.

In cement-based materials, Portland cement can be partially replaced by RHA due to its high silica content, minimal impurities, and pozzolanic properties [8], [9]. Several studies have demonstrated that substituting RHA for cement, typically around 10-15%, positively impacts the mechanical performance and durability of concrete [9]–[12], reducing production costs and CO_2 emissions [10], [13]. Ozturk et al. [14] studied the sustainability aspects of incorporating RHA into concrete production, concluding that this practice reduced CO_2 emissions by 25% and resulted in a 65% cost reduction. A detailed description of the possible RHA uses in the construction industry may be found in Jittin et al. [15] and Sandhu and Siddique [16].

Specifically, the use of RHA to partially replace Portland cement in self-compacting concrete (SCC) is vastly studied. Sandhu and Siddique [16] provide an insightful review of this subject. Their work reveals that the compressive, splitting tensile, and flexural strengths of SCC increase as RHA replaces cement up to 15%. This occurs due to the way the RHA improves the microstructure and pore structure of concrete due to its micro-filling and pozzolanic effects. They also remark that increasing RHA content in SCC decreases workability. However, the addition of a superplasticizer makes it possible to achieve improved workability and higher strength. Water absorption and porosity values decrease with RHA cement replacement by up to 30%. Incorporating RHA in SCC and blending it with other mineral additives improves the strength and durability of concrete. Several studies have investigated the effects of combining RHA with fly ash (FA), silica fume, metakaolin, limestone, hydrated lime, foundry sand waste, as well as agricultural wastes such as olive waste, bagasse ash, and sugarcane bagasse, among others, on the mechanical properties and durability of SCC [17]–[24].

The replacement of Portland cement by RHA on SCC can be accomplished by following two alternative procedures: (i) by establishing a value for workability and then adjusting either the high-range water-reducing admixture (HRWR) or the superplasticizer (SP) to reach this value; (ii) by defining the HRWR or SP content, and then measuring the workability of fresh concrete. Regardless of the chosen procedure, it has been demonstrated that such a replacement can enhance the SCC's mechanical performance and durability.

Following procedure (i), Raisi et al. [25] investigated the partial replacement of cement with RHA (in increments from 0% to 20%, increasing by 5% every step), as well as the effects of aged concrete, and the water-to-binder ratio. Their findings revealed that the passing and filling ability of SCC containing RHA decreases with an increase in the replacement ratio of RHA. Hence, in order to achieve satisfactory workability, more superplasticizer should be utilized. In contrast, the compressive strength, modulus of elasticity, and splitting tensile strength demonstrate an increase with up to 5% replacement of RHA. In Raisi et al. [26], the same authors also studied the fracture properties of SCC with RHA substitution, finding a reduction in both the concrete post-peak behavior and fracture energy with increased incorporation of RHA. The fracture toughness (K_{IC}) increases with the percentage of RHA replacement up to 5%, after which it begins to decrease, exhibiting similar behavior to other mechanical parameters.

Sathurshan et al. [27] studied cement replacement by RHA in 5% increments, ranging from 0% to 30%, along with varying percentages of fly ash (10%, 20%, and 30%). They increased the HRWR used to achieve the slump flow of around 600 mm and the V-funnel range between 6 and 12 s. The study revealed that higher dosages of admixtures were necessary to maintain the desired slump due to the increased viscosity caused by the incorporation of RHA, attributed to its high surface area and increased fraction. The only mix that does not have good fresh performance is the one with 25% of RHA replacement. The substitution of Portland cement for RHA up to 15% increases the compressive and splitting tensile strengths, whereas further incorporation of RHA decreases strength relative to the control specimen.

Diniz et al. [18] investigated the utilization of various supplementary cementitious materials (RHA, sugarcane bagasse ash, and metakaolin MK) in the production of SCCs, with the addition of hydrated lime and cement replacement up to 60%. They found that incorporating RHA-optimized viscosity contributed to control cohesion and reduced the bleeding of fresh concrete. However, as the other researchers found, a higher superplasticizer content was necessary to maintain the spread equivalent to the reference concrete. All mixtures containing RHA exhibited higher compressive strengths compared to the reference mix. Kannur and Chore [28] investigated mixtures ranging from 0% to 50% RHA in increments of 10%, finding that the highest compressive and splitting tensile strength values are obtained at 20%. Also, the HRWR dosage was fixed based on trials to attain the required fresh properties of SCC with a slump flow of around 650 mm. As the RHA content increased, higher superplasticizer dosages were required to achieve the specified workability. They also observed a reduction in water absorption and permeability as RHA content increased up to 20% across all curing periods up to 90 days. However, with RHA levels above 20%, the SCC specimens were found to absorb more water and increase the permeability during all curing periods.

Between the works that define the content of the HRWR or the SP, Safari et al. [29] tested the effect of RHA (0–8%) and macro-synthetic fiber (0–0.3%) on the properties of self-compacting concrete. They found that the RHA reduces the bleeding and increases the viscosity of the SCC paste. They also found a nonlinear effect on decreasing slump flow more intensively in higher percentages. At 28 days, the mix with 4% RHA demonstrated the highest compressive strength, while the mixture with 8% RHA showed the highest long-term compressive strength at 90 days. Ameri et al. [30] utilized a 2.5% superplasticizer in all mixes, increasing the content of RHA from 0 to 30% in 5% increments. The mixtures also had constant values of limestone powder and micro-silica. After performing the experiments, they determined that using 15% RHA yielded the optimal mix. The presented results of slump flow, V-funnel U-flow, and L-box tests confirmed the adverse effect of RHA on SCC's filling and passing ability. Their findings indicated that the compressive strength reaches a maximum value at 15% RHA content, with lower values observed for the 25% and 30% mixtures compared to the reference. Furthermore, the splitting tensile strength showed similar behavior.

Finally, Ameri et al. [30] revealed that water absorption, porosity, and water permeability decreased with increasing RHA content up to 15%, after which they began to increase. Hakeem et al. [19] also observed a decrease in slump with increasing RHA content. They noted that the compressive strength increased by approximately 13.6%, 22.5%, 32.8%, 41.1%, and 31.2% for RHA replacements of 5%, 10%, 15%, 20%, and 25%, respectively. Similarly, the splitting tensile strength also increased by 4%, 6.67%, 13.33%, 22.67%, and 8%, respectively, compared to the control mix.

In this context, the present work aims to experimentally investigate both the rheological properties (flowability, viscosity, and passing ability) and the mechanical properties (compressive and tensile strength) of a SCC incorporating fly ash (FA) and RHA, with the RHA used to replace Portland cement (PC). Specifically, the study examines various concrete mixtures with different percentages of RHA content, replacing 0% (plain concrete used as reference), 5%, 10%, 15%, 20%, and 25% of PC by weight proportion. Additionally, testing is conducted on hardened mixtures at various curing ages, accompanied by a comparative analysis with experimental data available in the literature.

2 EXPERIMENTAL STUDY

The present section covers the properties of the materials used to produce the SCC with FA incorporating RHA, along with the procedure employed for the mixture design. Subsequently, it describes the tests conducted in both fresh and hardened states.

2.1 Materials

2.1.1 Cement

The Brazilian Portland cement PC V-ARI-RS is used here [31]. This cement has a specific area of 4719 cm^2/g. The significant features of such a cement, defined by the producer, are a specific mass of 2.98 g/cm^3, a surface area of 1700 m^2/kg, and an average compressive strength of 48.3 MPa at an age of 28 days when a water/binder ratio equal to 0.45 is employed.

The particle size distribution is determined by using the Malvern laser granulometry equipment (Mastersizer 2000 model), which is reported in Figure 1a along with the addition curves, for better visualization of the grain size distribution. The distribution is carried out by a wet dispersion using Ethanol dispersant and performed in a range of particle sizes from 0.02 μm to 2000 μm. Figure 2a depicts a scanning electron microscopy (SEM) image of the cement powder, featuring a cement grain with a rough surface and irregularly shaped bumps.

It is noteworthy that CP V-ARI-RS is the cement with the lowest clinker replacement rate produced in Brazil and is the closest to Portland cement internationally produced, being chosen due to its minimal additions. It also has granulometry compatible with the other agglomerating materials and faster responses regarding the pozzolanic activity given by RHA.

2.1.2 Rice Husk Ash

The RHA used is a commercially available product [32]. The material is produced through a rice husk combustion process in a fluidized bed under a controlled temperature below 750 °C. The chemical composition of the RHA obtained by X-ray fluorescence (XRF) on a Shimadzu XRF 1800 sequential spectrometer and the fire loss values are shown in Table 1.

The RHA phase composition was determined using X-ray diffraction (XRD) with a 2θ Philips brand X'pert MPD diffractometer and analyzed through X-pert Highscore using the ICSD database. Figure 1b displays the XRD patterns, revealing a composite structure of a crystalline/amorphous phase. The halo ring observed at $18° < 2\theta < 30°$ is attributed to amorphous silica, while the peaks at $2\theta = 21.89°$ and 36.02° correspond to the crystalline cristobalite phase. This is likely related to contamination by the wind-blown sand of RHS during the fluidization process [33]–[35].

Table 1. Chemical composition of rice husk ash.

Composition	Component
Lost of fire	3.50%
Silicon Dioxide - SiO_2	91.48%
Silicon Dioxide - CaO	0.36%
Magnesium Oxide - MgO	0.32%
Iron Oxide - Fe_2O_3	0.05%
Aluminum Oxide - Al_2O_3	0.00%
Sodium Oxide - Na_2O	0.04%
Potassium Oxide - K_2O	1.40%
Manganese Oxide - MnO	0.32%
Sulfuric Anhydride - SO_3	0.15%
Diphosphorus Pentoxide - P_2O_5	0.45%

The utilized RHA presents a specific mass of 2.16 g/cm^3, a 21142 m^2/kg surface area, and a pozzolanic activity index of 0.92. This index represents the ratio of the average strength at 28 days for specimens molded with both cement and pozzolanic material and of specimens cast only with cement [36]. The fixed calcium hydroxide content, equal to 830 mgCaO/gSCA, is obtained through the modified Chapelle method [37], [38]. Through Brazilian standards [37] the pozzolanic activity of RHA was determined, finding 1379.37 milligrams (rng) of $Ca(OH)_2$ per gram (g) of material, thus characterizing that the material has pozzolanicity.

The granulometric distribution is determined by using the Malvern laser granulometry equipment (Mastersizer 2000 model) and reported in Figure 1a, with the Portland cement and fly ash curves. This distribution is carried out by wet dispersion using an Ethanol dispersant and performed in a particle size range from 0.02µm to 2000µm. Figure 2b shows an RHA powder SEM image. The figure illustrates that the RHA exhibits a grain size similar to that of cement (Figure 2b), albeit with a more porous and rough surface characterized by swells and irregular cavities. This coincides with the RHA description, multilateral, angular, microporous surface and honeycombed structure that justifies its high specific surface area [12], [16], [39].

2.1.3 Fly ash

The fly ash (FA) is obtained from the combustion of mineral coal at the Presidente Médici thermoelectric plant in Candiota, Brazil. The chemical composition of FA is referenced in [40]. The specific mass of the FA used is 1.98 g/cm^3. The granulometric distribution is determined by using the Malvern laser granulometry equipment (Mastersizer 2000 model) and is presented in Figure 1a. This distribution is achieved through wet dispersion using an Ethanol dispersant and performed in a particle size range from 0.02µm to 2000µm. Figure 2c shows an FA powder SEM image of the FA, revealing grains that are clumped spheres or rounded in shape.

Figure 1a reveals that RHA and PC V-ARI-RS exhibit a very similar granulometric distribution. However, RHA presents a slightly higher dispersion relative to its average diameter compared to cement. FA exhibits larger diameters than both RHA and cement, so filling voids between binder materials and fine aggregate.

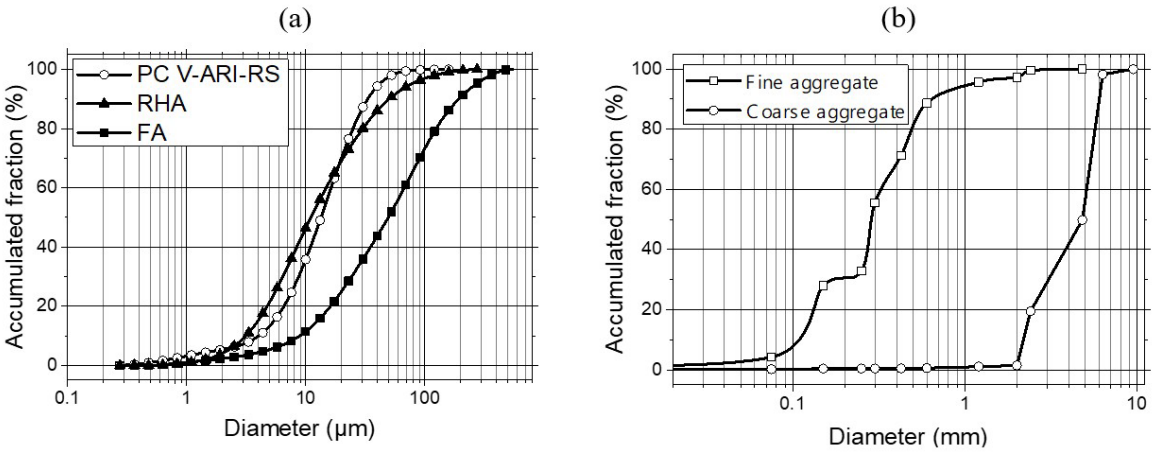

Figure 1. (a) Comparison between the granulometric curves of the binding material, PC, RHA and FA and (b) aggregate particle size distribution.

2.1.4 Aggregates

Quartz river sand from the central region of Rio Grande do Sul, Brazil, is utilized as fine aggregate, characterized by a maximum diameter of 2.40 mm, a fineness module of 2.06, a specific mass of 2.56 g/cm^3, and water absorption of 0.81%. Coarse aggregate (gravel 0) of basaltic origin is used, also originating from the central region of Rio Grande do Sul. The physical characteristics of the coarse aggregate used are a maximum diameter of 9.50 mm, a fineness module of 5.79, a specific mass of 2.70 g/cm^3, water absorption of 3.94%, and a unitary mass of 1.33 g/cm^3. Figure 1b depicts the particle size distribution of these two types of aggregates.

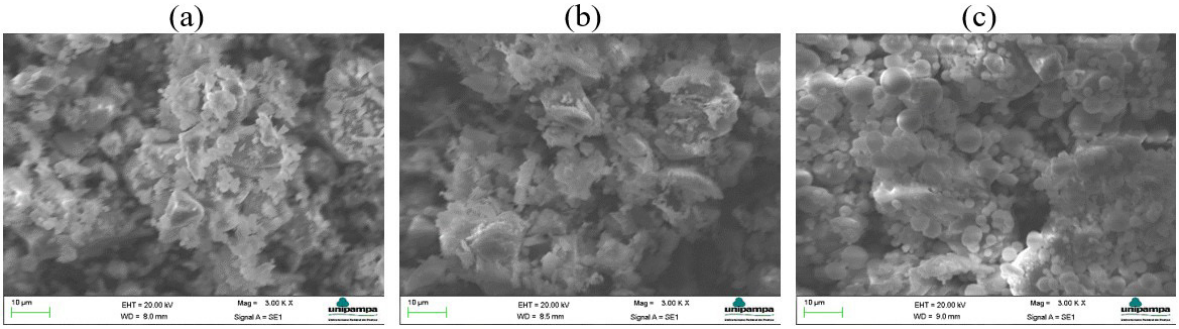

Figure 2. SEM pictures of powder of (a) PC V-ARI-RS cement, b) RHA, and c) FA, all recorded at a magnification of 3.00 K X (bar 10 μm).

2.1.5 Admixtures

A polycarboxylate-based dispersant is used as a superplasticizer. It has a 30.0% solid content, a specific mass of 1.073 g/cm^3, and PH 6.2, as reported by the producer. During the concrete manufacturing, a powdered viscosity modifying agent (VMA), Rheomac UW 410 (produced by BASF), is added to the wet mixture.

2.2 Concrete mix design

Different methods of dosage can be used to define the concrete mix, as reported by Tutikian and Pacheco [41]. In this study, the mix design follows the approach proposed by Gomes [42], aiming to obtain a high-strength self-

compacting concrete. According to this method, mix design is obtained by separately optimizing the cement paste composition and the granular skeleton. The method is performed in three phases:

- Obtaining the composition of the paste, which involves determine the superplasticizer (sp) dosage relative to the cement mass, sp/c to achieve a paste with excellent properties for SCC.
- Establishing the proportion of aggregates by measuring the dry density of their mixture, using a modified experimental method based on ASTM C29/C29M standard [43].
- Determining the paste volume that provides a concrete with the self-compacting requirements, assessed in terms of filling ability, ability to pass through obstacles, and resistance to segregation.

2.2.1 Paste composition definition

The paste composition is related to the amount of cement, C, and the ratios of the other components of the paste as a function of the cement mass, such as water (w/c), superplasticizer (sp/c), and fly ash (fa/c). The equations used to obtain the paste are: $P_w = (w/c)\,C$, water mass; $P_{fa} = (fa/c)\,C$, fly ash mass; $P_{sp} = (sp/c)\,C$, mass of solid superplasticizer; $P_{spl} = P_{sp}/(T_{sp}/100)$, mass of liquid superplasticizer, and $P_{wsp} = P_{sp}\left[\left(100/T_{sp}\right) - 1\right]$, water mass content in the superplasticizer, where T_{sp} is the solids content on the superplasticizer. The added real water mass is corrected by subtracting the water contained in the superplasticizer. So, the corrected mass of water is $P_{wc} = P_w - P_{wsp}$. The paste volume is obtained by Equation 1:

$$V_p = \frac{C}{\rho_c} + \frac{P_w}{\rho_w} + \frac{P_{fa}}{\rho_{fa}} + \frac{P_{spl}}{\rho_{sp}} - \frac{P_{wsp}}{\rho_w} \tag{1}$$

Based on the work of Marangon [44], 15% of mass of fly ash was added to enhance the workability of the concrete in the fresh state and achieve a more cohesive mixture. With this assumption, the binder is defined as the sum of the cement and the fly ash contents, $b = c + fa$.

According to Brazilian standards, sulfate-resistant cement such as PC V ARI-RS must be used in concrete exposed to severe aggressive conditions, with a maximum water/cement ratio of 0.45 in mass, in concrete with normal aggregate. Therefore, the water/binder ratio, w/b, of 0.45 was employed, considering the highest aggressiveness class that the concrete may encounter. The optimal superplasticizer dosage (sp/c ratio) is determined through tests and parameters described below.

The superplasticizer dosage is determined by measuring the time required for one liter of fluid to flow through the Marsh funnel with a 5 mm diameter. Measurements of paste flow time are taken at intervals of 5, 30, and 60 minutes to assess variations over time. The flow time test for evaluating paste flow characteristics was conducted using a water-to-binder ratio of 0.45.

The results demonstrate that the superplasticizer is compatible and efficient in dispersing the particles of the materials used to compose the concrete. Figure 3a shows flow time versus dispersant content curves relative to compatibility tests performed on cement pastes.

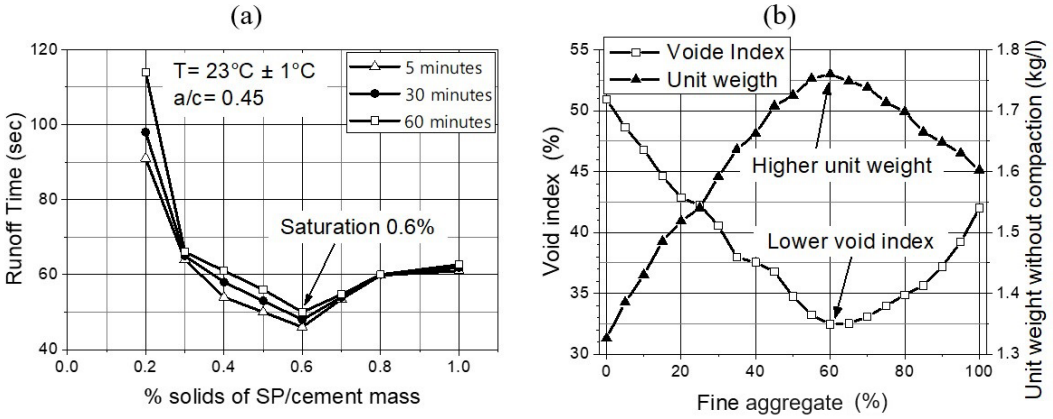

Figure 3. (a) Saturation curves of PC V ARI-RS cement. (b) Ratio of the lowest void rate versus percentage of fine aggregate.

As can be seen in Figure 3a, a superplasticizer content of 0.6% represents the saturation point. Figure 3a also illustrates a well-defined optimal point for superplasticizer dosage in the pastes, with internal angles of the curve at the saturation point as established by Gomes [42], i.e., 140° ± 10°.

2.2.2 Granular skeleton

A granular skeleton is the composition of coarse and fine aggregates that comprise concrete. The selected composition is obtained experimentally by measuring the density of dry, uncompacted aggregate mixtures and selecting the composition that achieves the highest density and lowest void content.

The procedure consists of manually joining the aggregate mixtures in a mixer and placing them in a container of known volume without any compaction. The apparent density, or unit weight, of various combinations is then measured by varying the percentage ratio between fine and coarse aggregates to determine the void content. The unit weight and void volume of each mixture are calculated using the densities and weights of the aggregates, as illustrated in Figure 3b.

As shown in Figure 3b, the ratios found for the lowest volume of voids between the fine and coarse aggregates were 60% and 40%, respectively, resulting in the highest unit mass over the mixtures (1.768 kg/l).

2.2.3 Determination of the paste volume

Once the paste composition and granular skeleton are defined, the final parameter needed to establish the concrete composition is the paste content (or alternatively, the aggregate content) per volume. This parameter is determined through tests where the paste volume is varied to achieve the desired properties for self-compacting concrete. According Gomes [42], this procedure considers that the paste volume must be sufficient to fill the voids between the aggregates and ensure the separation distance between the aggregate particles.

The Brazilian standard [45] specifies that concrete mixes for classes C10 and C15 can be empirically established, requiring a minimum of 300 kg of cement per cubic meter. SCC is considered a specialized type with a high proportion of fine materials, hence 350 kg of PC per cubic meter was used in the reference concrete. Once the cement content is determined, the paste volume and all other components can be calculated using Equation 1. A paste volume of 325.8 l/m^3 was found. The composition of the reference mixture is presented in the first column of Table 2.

2.2.4 Mix definition

The composition of aggregates in the concrete is chosen from the smallest volume of voids between the fine and coarse aggregates. This is found in the granular skeleton with 60% of fine aggregate (sand) and 40% of coarse aggregate. As previously mentioned, a water/binder ratio of 0.45 was employed for the concrete mix. Based on Marangon [44], 254 ml of VMA was used per m^3 of concrete. The SCC mix obtained by the method of Gomes [42] is presented in the first column of Table 2, C00.

Six mixtures were analyzed to investigate the effect of adding RHA on concrete mixes, each incorporating a 15% mass addition of FA relative to the weight of binders. These mixtures replaced 0% (plain concrete used as a reference), 5%, 10%, 15%, 20%, and 25% of PC by RHA. These defined mixes and the amounts of cement and RHA used in each mix are presented per m^3 of concrete in Table 2. This table also provides the nomenclature used for each analyzed mixture throughout the study.

Table 2. SCC mix composition obtained by the method of Gomes [42], consumption of materials per m^3 of concrete (kg/m^3).

Material (kg)	Mixture					
	C00	**C05**	**C10**	**C15**	**C20**	**C25**
Cement	350.00	332.50	315.00	297.50	280.00	262.50
RHA	0.00	17.50	35.00	52.50	70.00	87.50
Fly ash	61.77	61.77	61.77	61.77	61.77	61.77
Fine aggregate	1059.52	1059.52	1059.52	1059.52	1059.52	1059.52
Coarse aggregate	706.35	706.35	706.35	706.35	706.35	706.35
Water	179.53	179.53	179.53	179.53	179.53	179.53
Superplasticizer	8.24	8.24	8.24	8.24	8.24	8.24
VMA	0.25	0.25	0.25	0.25	0.25	0.25

Each SCC mix presented in Table 2 was prepared using a concrete mixer with an inclined axis, primed with a 1:2 cement and sand mortar. The materials were added in a consistent sequence for all mixtures, with the mixer in motion, following this order: 100% coarse aggregate (crushed stone) with 30% water; 100% binder materials (cement and fly ash); 100% RHA; 70% water plus superplasticizer; 100% fine aggregate (sand); and 100% VMA.

After the 5-minute mixing period, all tests on the fresh concrete were conducted. Curing of all specimens began in air for the first 24 hours after molding. Then, the specimens were demolded and placed in an immersion tank at a temperature of 21±2°C, remaining there until the testing dates.

2.3 Test procedures

This section presents the methods employed to test the various mixtures in both fresh and hardened states.

2.3.1 Fresh concrete testing

All tests were conducted in accordance with Brazilian standards [46] and EFNARC guidelines [47]. Specifically, flowability was assessed using the slump-flow test. Viscosity measurements were obtained through both the T500 slump-flow test and the V-funnel test, which also provide insights into SCC's flowability. Passing ability was evaluated using the L-box, J-ring, and U-box tests. Additionally, the J-ring test was utilized to measure SCC's flowability. It is important to note that each test was performed only once for each mixture.

In this study, segregation resistance was not directly measured because, as defined in [47], segregation resistance becomes a significant parameter in higher slump-flow classes or lower viscosity classes. Specifying a segregation resistance class is typically unnecessary if these conditions do not apply. However, additional information on segregation resistance and concrete uniformity can be obtained by the visual observation during the slump flow test, as conducted in this study.

2.3.2 Hardened concrete testing

The axial compressive and splitting tensile strengths were determined according to Brazilian standards [48], [49].

Compression tests were conducted on the six mixtures listed in Table 2 at curing ages of 7, 28, 56, and 91 days. More precisely, five cylindrical specimens, each with a diameter of 10 cm and height of 20 cm, were molded for every mixture and curing age (Table 2). The specimens were compacted in two layers, with 12 strokes per layer, using a cylindrical shank measuring 16 mm in diameter and 600 mm in length, with a hemispherical end. Initially, curing occurred for 24 hours with the concrete remaining inside the molds. Subsequently, specimens were demolded and placed in an immersion tank until the scheduled test dates. The compression tests were performed using an EMIC PC150 machine, with a loading speed of 0.50 MPa/s, equipped with a load cell capacity of 1.5 MN.

Splitting tensile tests were conducted on five cylindrical specimens for each of the six mixtures listed in Table 2. Each specimen had a diameter of 10 cm and a height of 20 cm, and tests were performed at curing ages of 7, 28, 56, and 91 days. The tests were performed using a Universal Testing Machine, specifically the EMIC DL20000 model, with a loading speed of 0.05 MPa/s and equipped with a 200 kN capacity load cell.

3 RESULTS AND DISCUSSIONS

In this section, the results obtained, both in terms of rheological and mechanical properties, are presented and discussed.

3.1 Flowability

The results obtained by the slump-flow tests for each concrete mixture examined are listed in the first line of Table 3. This table presents the results obtained on SCC’s fresh state tests.

It can be observed that the spreading flow diameter ranges from 645 mm (C25 mixture) to 680 mm (C00 and C15 mixtures), representing the average value of two measured diameters for each flowing concrete sample. Figure 4a illustrates the spreading flow diameter for each mixture, along with the corresponding Slump-Flow classes (SF1 – 550 to 650 mm; SF2 –660 to 750 mm; SF3 – 760 to 850 mm) [46], [47].

It is noticeable that the spreading flow diameter generally decreases by increasing the RHA content. Moreover, according to EFNARC guidelines and Brazilian standards [46], [47], the mixtures from C00 to C15 are classified as SF2, which are stable enough to be employed building walls, beams, and columns. In contrast, C20 and C25 mixtures are classified as SF1, suitable for housing slabs, tunnel linings, piles and some deep foundations.

Table 3. Results obtained from SCCs in the fresh state.

Mixture	C00	C05	C10	C15	C20	C25
Slump-flow (mm)	680	680	670	675	650	645
T_{500} Slump-flow (s)	6.0	6.0	5.5	5.5	7.0	8.0
V-Funnel (s)	12.5	10.5	10.0	10.5	13.0	14.5
L-Box (H2/H1)	0.80	0.82	0.85	0.84	0.85	0.83
J-Ring (mm)	25	30	25	30	15	15
U-Box (R1-R2)(mm)	5	6	7	7	9	10

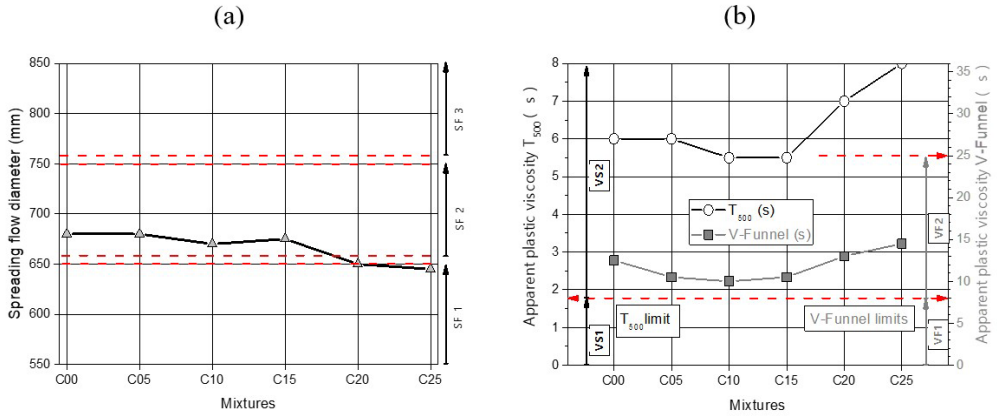

Figure 4. (a) Spreading flow diameter obtained on slum-flow test for each mixture analyzed. (b) Apparent plastic viscosity T500, and V-Funnel, for each of the mixtures studied.

3.2 Viscosity

The results obtained by the T500 slum-flow test and V-funnel test for each concrete mixture examined are listed in the second and third lines of Table 3. All tests were filmed, and the times shown in Table 3 are obtained from the recordings.

It can be observed that the apparent plastic viscosities obtained with both tests have the same behavior. For small replacements (C05, C10, and C15 mixtures), the viscosity tends to decrease, and for a higher content of RHA, it increases again. It is important to note that each mixture underwent only one test, and any observed differences would fall within typical result variations. However, both methods found the highest viscosity for mixtures with 10-15% RHA.

Figure 4b shows the apparent plastic viscosity obtained with T500 slump-flow and V-funnel tests for each of the mixtures analyzed. This figure also presents the viscosity classes defined by the Brazilian standards [46] and EFNARC guidelines [47].

As depicted in Figure 4b, the behavior of the two curves is similar, confirming the accuracy of the results obtained through different methods. In this case, there is no change in the concrete classification, VS2/VF2, when replacing RHA for PC.

3.3 Passing ability

The results obtained by the L-Box test, the J-Ring test, and the U-Box test for each concrete mixture examined are detailed in the fourth, fifth, and sixth lines of Table 3, respectively. It is noteworthy that higher values in the L-Box and J-Ring tests indicate greater passing ability of the concrete. Conversely, a lower result in the U-Box test suggests higher passing ability.

It can be observed that the passing ability measured by the L-Box test tends to stabilize for replacements exceeding 10% and begins to decrease with amounts around 25%. All mixtures with replacements are shown to have more passing ability than the reference with this method. The J-Ring test results exhibit a comparable trend, although mixtures with 20% and 25% replacements demonstrate lower passing ability than the reference. The results of the U-Box test decrease as the replacement percentage increases, indicating a widening difference between R1 and R2. Therefore, the mix presents less passing ability with increasing RHA. Figure 5a illustrates the behavior of L-Box results with different replacement amounts of PC by RHA, alongside with the passing ability measured with the J-Ring test.

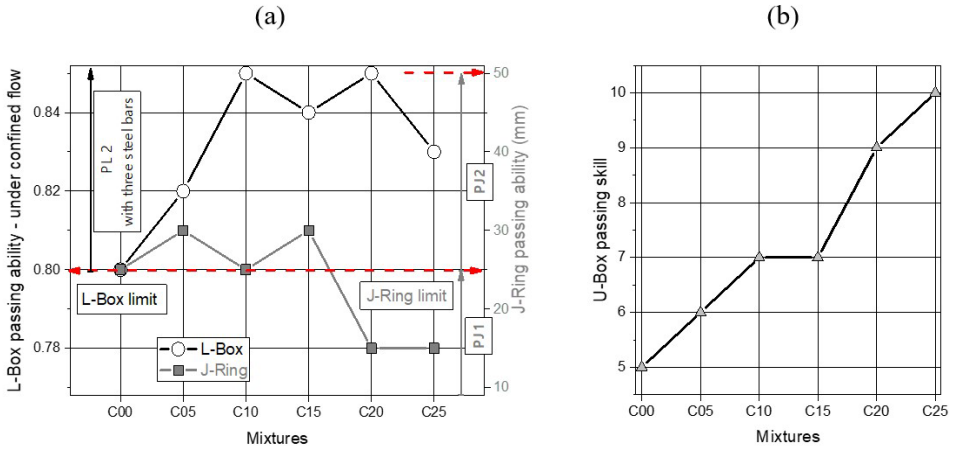

Figure 5. Passing ability obtained by: (a) L-Box and J-Ring, (b) U-Box, for each of the mixtures studied.

As shown in Figure 5a, following the Brazilian standard [46], all concretes maintained the same classification for the L-Box test, except for those with 20% and 25% PC replaced by RHA, which experienced a classification change. As previously demonstrated, the slump-flow test also showed a classification change for these same mixtures. This alteration occurs because, at these RHA proportions, the concrete becomes more viscous, resulting in reduced fluidity and passing ability.

Figure 5b illustrates the findings from the U-Box test, where all results are notably lower than the 30 mm threshold suggested by the Brazilian standard [46]. As described before, the results of the U-Box test contradict those obtained with the L-Box and J-Ring tests, indicating that passing ability diminishes with increasing RHA content. The previous two tests showed that this property initially improves and then begins to decline.

3.4 Segregation

As previously defined, segregation resistance becomes an important parameter, particularly in higher slump-flow classes or lower viscosity classes, although not applicable to the concrete mixtures studied here. Figure 6 shows the pictures of the J-Ring test conducted on all concrete mixes examined in this work. It is possible to observe that all formulations exhibited excellent water retention and no signs of segregation, as depicted in Figure 6.

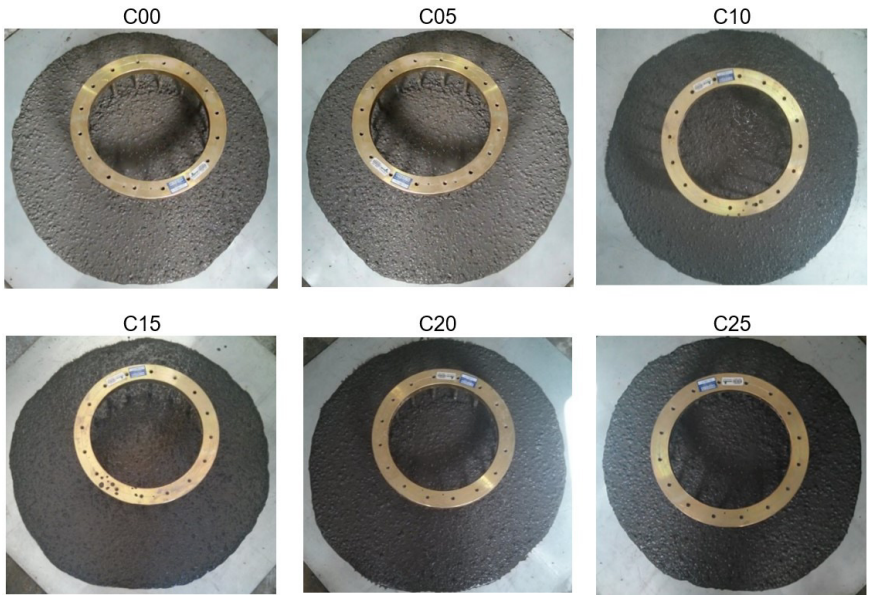

Figure 6. Photographs of scattering obtained from the J-Ring test on every mixture of the SCC studied.

3.5 Compressive strength

The results obtained by the axial compression tests are listed in Table 4 for each concrete mixture and curing age examined. This table includes the mean axial compressive strength, f_c, and the coefficient of variation, CV, for each tested condition.

As shown in Table 4, the average axial compressive strength of the C00 mixture at 7 curing days surpasses that of the other SCC mixtures, driven by the rapid water reaction characteristic of PC V ARI – RS cement, which achieves high early-stage strength. At 28, 56, and 91 days, all mixtures except C10 exhibited strengths above the reference concrete. This slower reaction of RHA silica particles with calcium hydroxide (CH), produced during cement hydration, along with RHA's fine particle size, enhances nucleation of crystals and strengthens the material. According to several authors and highlighted in the review by Fapohunda et al. [10], this phenomenon is expected because mixtures produced with partial replacement of PC by RHA experience significant strength gains over time, as the pozzolanic material requires CH and water to react. So, in the first days, PC reacts with water and forms CSH+CH. This CH, in the presence of pozzolanic materials (RHA and FA) and water, develops additional hydration products, i.e., additional CSH.

Table 4. Average values and coefficients of variation of the axial compressive strength, f_c.

Mixtures	7 curing days	28 curing days	56 curing days	91 curing days
	f_c (MPa) – CV (%)	f_c (MPa) – CV (%)	f_c (MPa) – CV (%)	f_c (MPa) – CV (%)
C00	25.73 – 5.80	34.17 – 2.91	38.22 – 5.26	47.39 – 4.80
C05	24.86 – 3.28	35.36 – 1.11	46.93 – 2.77	49.79 – 2.81
C10	21.06 – 5.80	30.51 – 2.91	37.67 – 5.26	45.58 – 4.80
C15	23.70 – 2.63	36.61 – 1.09	46.16 – 2.31	53.53 – 2.35
C20	20.09 – 0.91	32.61 – 3.52	45.21 – 0.78	50.80 – 1.65
C25	20.52 – 1.84	33.18 – 1.25	43.48 – 2.57	52.04 – 1.87

Figures 7a to 7d shows the mean values of axial compressive strength for each mixture and for curing ages of 7, 28, 56, and 91 days, respectively. Figure 7 presents the mean strength of the reference concrete at 28 days of curing to facilitate comparison. Additionally, it includes a highlighted region, between dotted lines, with three standard deviations of the means, ±1.41 MPa, related to the mean strength of the C00 mixture at every curing age. If the mean value of a mixture falls within this highlighted region, it indicates no statistically significant difference compared to the reference mixture at the corresponding curing age.

In Figure 7a, it is possible to verify that there is no statistically significant difference between the axial compression strengths at 7 days between mixtures C00 and C05. Additionally, at this curing age, there is a decrease in compressive strength as the replacement percentage increases. As discussed earlier, at this curing age, there was not enough time for the reaction of calcium hydroxide (CH), formed in cement hydration, with RHA.

Figure 7b illustrates the mean axial compressive strengths of SCCs after 28 days of curing. At this age, there are no statistically significant differences in the mechanical strengths of axial compression between the mixtures C00, C05, C20, and C25. The C10 mix has a slightly lower resistance than the reference one, while the C15 mix is slightly higher. Overall, there is virtually no change in axial compressive strengths with increased cement replacement by RHA at 28 days.

Figures 7c and 7d indicate that at both 56 and 91 days of curing age, there is an increase in axial compressive strength compared to the reference concrete for all mixtures studied. The only exception is the C10 mix, which exhibits different behavior. These figures also demonstrate that as the replacement amounts increased, the axial compressive strengths for SCC produced with RHA improved at 56 and 91 days. However, although the C10 mixture also increased, it remained with a lower strength than the C00 mix.

Figure 8 also compares the average compressive strengths of each mixture at every curing age studied. To facilitate comparison, the compressive strengths are normalized to the compressive strength of the reference mixture (C00) at 28 days, represented by the red dashed line.

As presented in Figure 8, the strength gain at 91 days, compared to the mix of 28 days, increases from 39% in the reference concrete to approximately 50% in the mixtures C05, C15, C20, and C25. Only the C10 mix had a lower gain compared to the reference mix. Additionally, it also reveals that while the reference mixture experienced an increase in resistance to rupture of 84% from 7 to 91 days. The substituted mixtures obtained 100%, 116%, 126%, 153% and 154% gains for C05, C10, C15, C20, and C25 respectively.

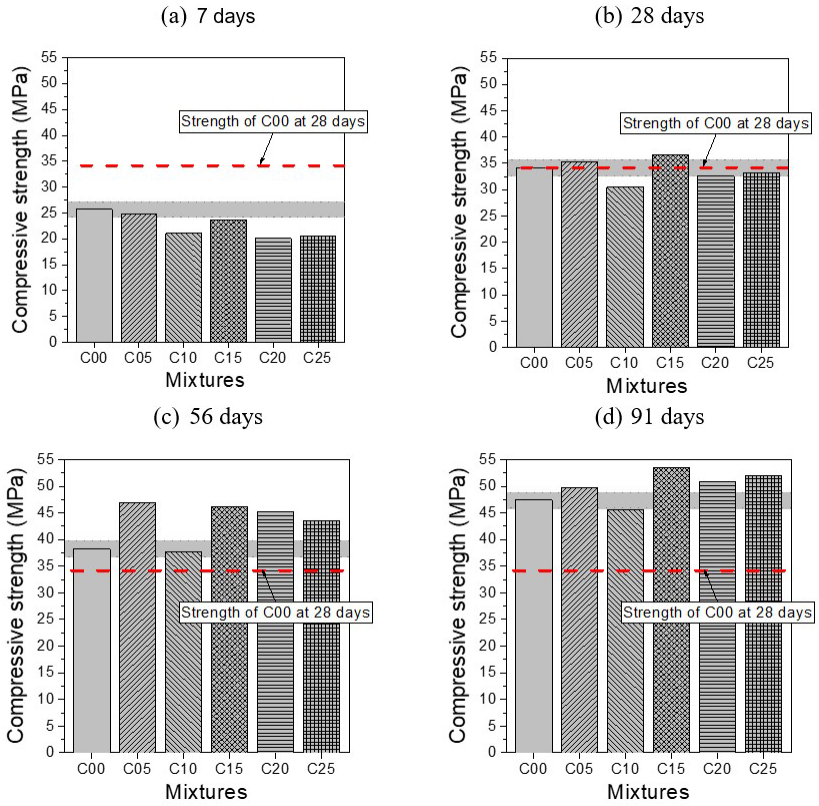

Figure 7. Multiple comparison of means of axial compressive strength at 7, 28, 56, and 91 days for the SCCs studied.

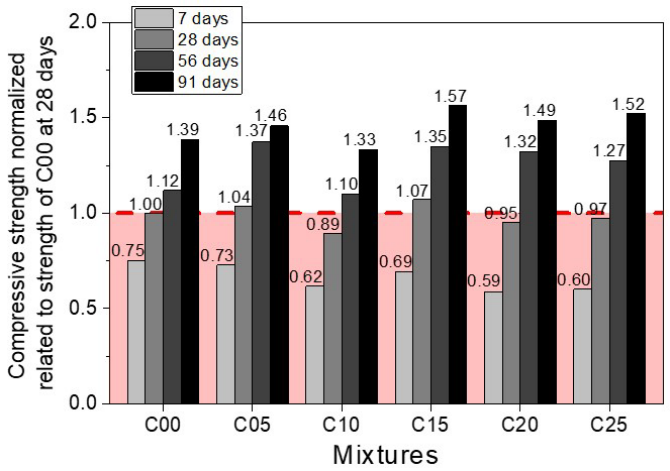

Figure 8. Comparison of compressive strength gain over age across different mixtures.

The amount of cement and the compactness of the mixture (decreases with increased substitution) influence the initial rate, which is referred to as cement hydration. Between 7 and 56 days, the pozzolanic effect of RHA seems to be decisive in the gain of resistance, that is, the consumption of CH. After 56 days, the increase is stabilized due to the pozzolanic of the FA present in all mixtures. Thus, all curves are expected to continue to present similar rates for older ages.

3.6 Splitting tensile strength

Table 5 lists the results of the splitting tensile test for each concrete mixture and curing age examined. More precisely, the mean value of the splitting tensile test, f_t, and the corresponding coefficient of variation, CV, are listed in the table.

Table 5. Experimental results of splitting tensile strength, f_t.

Mixtures	7 curing days	28 curing days	56 curing days	91 curing days
	f_t (MPa) – CV (%)	f_t (MPa) – CV (%)	f_t (MPa) – CV (%)	f_t (MPa) – CV (%)
C00	2.76 – 11.84	3.23 – 9.56	3.72 – 7.53	4.35 – 6.52
C05	2.84 – 8.29	3.76 – 6.60	4.06 – 8.94	4.13 – 6.27
C10	2.61 – 2.50	3.05 – 9.94	3.55 – 8.09	4.71 – 1.20
C15	2.67 – 7.67	3.42 – 5.95	4.01 – 8.35	5.20 – 3.62
C20	2.49 – 3.70	3.38 – 8.05	3.91 – 8.02	4.92 – 6.62
C25	2.30 – 3.34	3.18 – 7.36	4.09 – 5.48	5.23 – 8.09

Table 5 shows that the splitting tensile strength increases with curing age across all analyzed mixtures. Additionally, at any given curing age, the strength varies depending on the percentage of RHA in the mixture.

Figure 9 displays the average values of splitting tensile strength for each studied mixture at different curing ages, along with the mean value strength of the reference concrete at a curing age of 28 days to facilitate comparison. This figure also includes a highlighted region (between dotted lines) representing three standard deviations of the means, ±0.35 MPa, related to the mean strength of the C00 mixture at every curing age. If the mean value of a mixture falls within this highlighted region, it indicates no statistical difference between this mixture and the reference at the corresponding curing age.

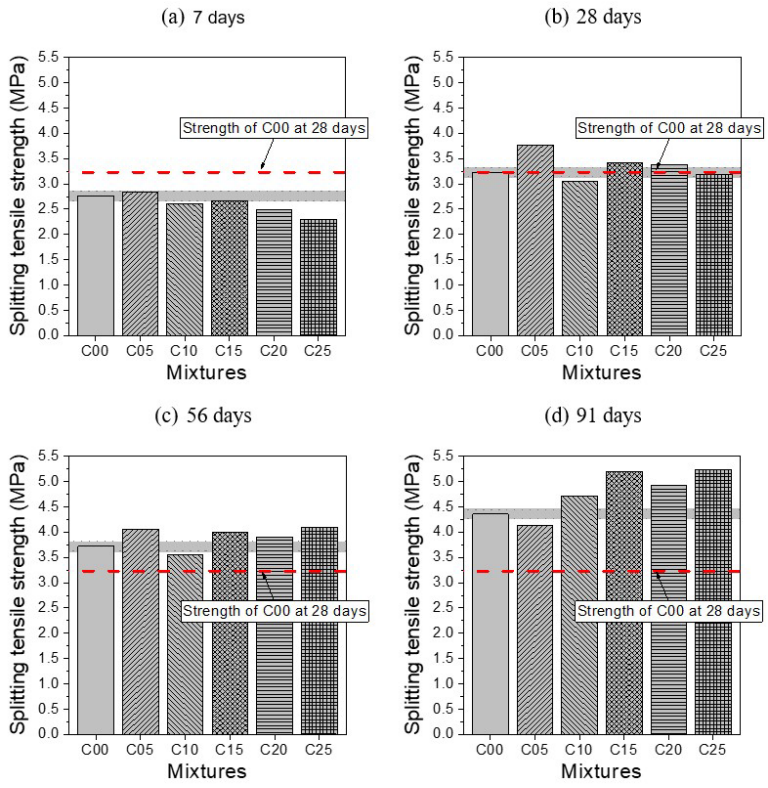

Figure 9. Multiple comparison of means of mean splitting tensile strengths at 7, 28, 56, and 91 days for the studied SCCs.

Figure 9a presents the results of the SCCs mixtures studied for a 7-day curing age. It is possible to verify that there is no statistically significant difference in the splitting tensile strength at 7 days between mixtures C00, C05, and C15 (all falling within the decision limit range of 3 standard deviations from the means). However, a notable decline in splitting tensile strength is observed with replacements exceeding 15%. This trend mirrors the findings in compressive strength, as discussed earlier.

Figure 9b illustrates the mean splitting tensile strengths at 28 days. At this age, there were no statistically significant differences between the C00 and C25 mixtures. As seen in Figures 9b, 9c and 9d, from 28 days onwards, the SCCs produced with the mixtures C15, C20, and C25 present splitting tensile strengths greater than C00, gaining more resistance the further it ages. The C10 mixture also demonstrated this inversion, albeit more gradually, eventually surpassing the strength of the reference concrete by 91 days. The C05 mix showed a well-differentiated behavior from the beginning. At 7 days, it had a splitting tensile strength higher than C00, and it increased significantly at 28 days. However, the rate of increase in splitting tensile strength began to decline thereafter, falling below that of the reference concrete by 91 days.

Figure 10 compares the average tensile splitting strength categorized by the percentage of replacement studied. To facilitate comparison, the tensile splitting strengths in this figure are normalized to the strength of the reference mixture (C00) at 28 days, represented by the red dashed line.

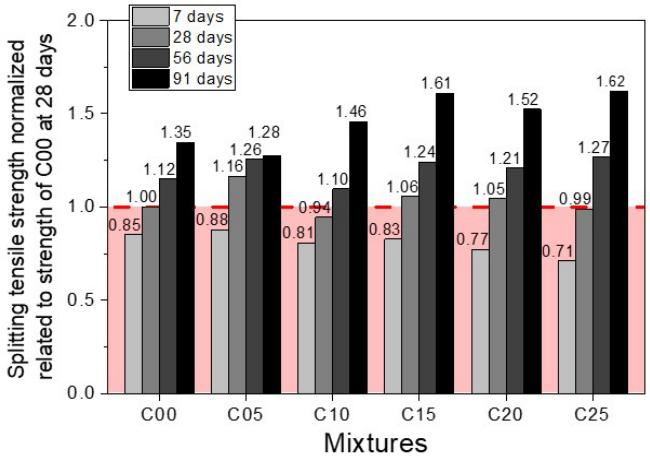

Figure 10. Comparison of splitting tensile strength gain over age across different mixtures.

In Figure 10, it is possible to observe that at 7 days, the strength gain, compared to the 28 days of reference mix, decreased with increasing substitution. This trend apparently occurred because there was not enough time for the reaction of calcium hydroxide (CH), formed in the hydration of the cement, to react with pozzolan (RHA). By 91 days, this pattern reverted, reaching gains of up to 30% when compared to the C00 mix. Additionally, the reference mixture achieved a 58% increase in strength from 7 to 91 days, whereas mixtures with replacements had increases of 45%, 81%, 95%, 97%, and 128% for mix compositions C05, C10, C15, C20, and C25 respectively. The C05 mixture has a lower result than the reference one, indicating less resistance increase.

4 COMPARISON BETWEEN THE RESULTS OBTAINED AND LITERATURE DATA

Figure 11 shows the axial compressive strength values compared to the splitting tensile strength for the different analyzed mixtures, alongside the limits suggested by the CEB-FIP code [50]. The upper limit is $f_t = 1.85(f_c/10)^{0.67}$, and the inferior limit is $f_t = 0.95(f_c/10)^{0.67}$, where f_t is the tensile strength, and f_c is the compressive strength.

As presented in Figure 11, in the reference mixture (C00), the resistances at 7 and 28 curing age (the lowest values) coincide with the average curve of the Code. However, as age increases, the obtained curve progressively approached the maximum limit. Similar behaviors are observed in mixtures with substitutions exceeding 5%, with this effect becoming more pronounced as the level of substitution increases.

In Figure 11, it is also noteworthy that in all mixtures aged 7 days (lower strengths), the average points obtained are close to the average curve of the CEB-FIP Code [48] without a pozzolanic effect. However, as age and resistance increase, the average values obtained in the tests deviate from the Code's average curve. It is important to point out that this also happens with the reference concrete, due to adding 15% of FA in the mixture, a material that also has pozzolanic properties.

The results obtained in this research agree with findings in the literature [9]–[12] regarding the use of RHA as a substitute for cement. Furthermore, around 10-15% of substitution has the best mechanical performance and durability of concrete. When compared with other studies that use RHA to partially replace PC in SCC, the results are also

compatible. The compressive and splitting tensile strengths increase with the replacement of PC content up to 15%, as presented in the review of Sandhu and Siddique [16]. They also remark that increasing RHA content in SCC reduces workability, the same result obtained in this work.

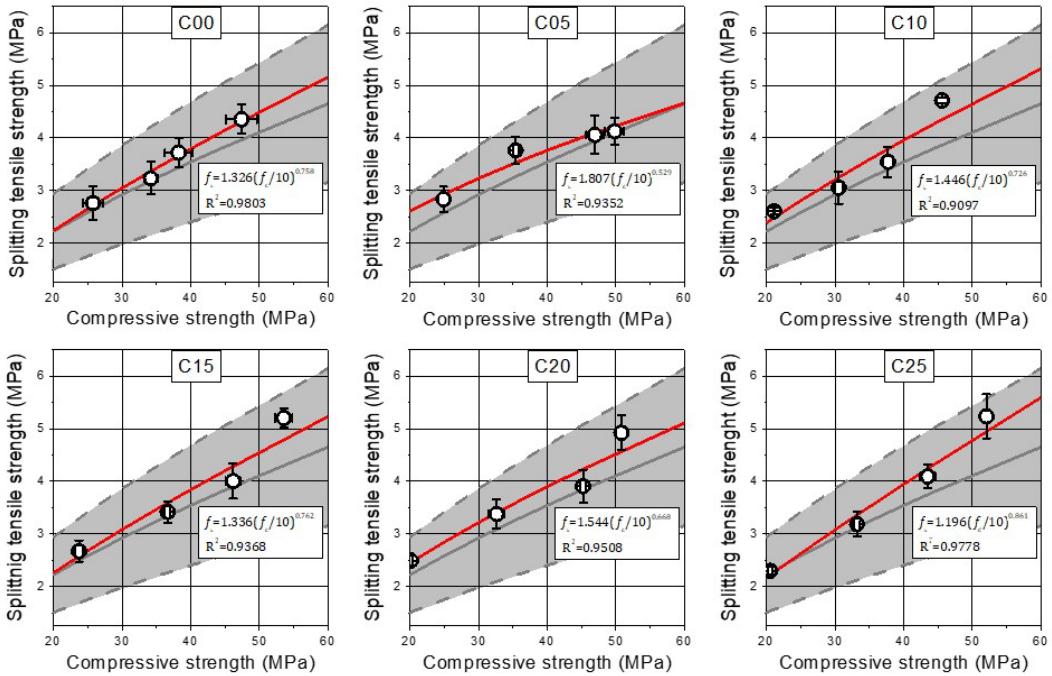

Figure 11 – Axial compressive stress versus splitting tensile strength compared to the limits suggested by the CEB-FIP code [50].

In this study, it was determined that the mixture with 15% RHA yielded optimal results. The same results were reported by Ameri et al. [30]. However, these authors observed lower values for replacements of 25% and 30% compared to the reference mixture, contrasting with our results. Our study aligned with the results reported by Hakeem et al. [19], indicating that replacements with more than 15% of RHA can enhance concrete strengths beyond those of the reference mixture. As observed by other researchers, it is noteworthy that the SCC's filling, passing ability, and its slump decreased with the RHA content increase.

It is possible to observe in this work that the ideal amount of replacement of PC by RHA is 15% since both the splitting tensile strength and the axial compressive strength for this mixture were the highest compared with the other mixtures. Additionally, it is important that for this mixture, there is no change in any classification of the fresh concrete state, presenting the same characteristics as the reference concrete. However, mixtures C20 and C25, which contain higher levels of replacement, also showed favorable mechanical properties surpassing those of the reference concrete. These mixtures can offer viable solutions when reduced fluidity or passing ability is necessary, given their cost-effectiveness and ecological benefits due to lower cement content and higher incorporation of waste materials.

5 CONCLUSIONS

This study explores the feasibility of using rice husk ash, produced under controlled burning conditions in a fluidized bed, as a partial replacement for PC V ARI-RS cement in the production of SCC for structural purposes. SCCs were investigated with RHA substitutions at 5%, 10%, 15%, 20%, and 25% of the cement content, and the addition of 15% of fly ash with w/b of 0.45. Tests assessing flowability, viscosity, and workability in the fresh state were conducted, alongside mechanical tests measuring axial compressive strength and splitting tensile strength in the hardened state.

Concrete with self-compacting characteristics was successfully produced using the method developed by Gomes [42]. Self-compacting concretes with varying levels of PC replaced by RHA have also been produced using previously mentioned dosages.

Regarding rheological properties in the fresh state, it was observed that increasing the replacement of PC with RHA resulted in decreased fluidity and passing ability characteristics of the concrete, although all mixtures exhibited self-

compacting properties. Concretes with replacements exceeding 15% showed altered flowability and passing ability classifications in the J-Ring test, which could restrict their application in certain structural elements. Moreover, higher levels of RHA replacement led to increased cohesion and viscosity of the concrete in its fresh state compared to the reference concrete. Based on the fresh state analyses, it has been concluded that minimizing PC replacement with RHA enhances the concrete's performance.

The hardening properties studied in this work have been improved with the replacement of cement by RHA compared to the reference mixture. On average, concrete with a 15% replacement exhibited the highest resistance. Mixtures with 20% and 25% replacement showed gains exceeding 10% compared to the reference at 91 days, reinforcing the idea that the optimal amount would be above 15% replacement.

The concrete with a 15% replacement of PC by RHA exhibits the highest axial compressive strength. However, 20% and 25% replacements would also be suitable as they perform well in the hardened state. Increasing the quantity of superplasticizer in the latter two mixtures can improve their fluid properties. From a strength perspective, concretes with 5% and 10% PC replacement by RHA are not recommended.

ACKNOWLEDGEMENTS

The present work was completed with the support of the Coordination for the Improvement of Higher Level Education Personnel (CAPES) and the National Council for Scientific and Technological Development (CNPq).

REFERENCES

[1] IRGA. https://irga.rs.gov.br/safras (accessed Mar. 8, 2024).

[2] A. R. Bodie, A. C. Micciche, G. G. Atungulu, M. J. Rothrock Jr., and S. C. Ricke, "Current trends of rice milling byproducts for agricultural applications and alternative food production systems," *Front. Sustain. Food Syst.*, vol. 3, pp. 47, 2019, http://doi.org/10.3389/fsufs.2019.00047.

[3] A. Abraham, A. K. Mathew, R. Sindhu, A. Pandey, and P. Binod, "Potential of rice straw for bio-refining: an overview," *Bioresour. Technol.*, vol. 215, pp. 29–36, 2016, http://doi.org/10.1016/j.biortech.2016.04.011.

[4] G. Tlaiji, S. Ouldboukhitine, F. Pennec, and P. Biwole, "Thermal and mechanical behavior of straw-based construction: a review," *Constr. Build. Mater.*, vol. 316, pp. 125915, Jan 2022, http://doi.org/10.1016/j.conbuildmat.2021.125915.

[5] B. Sangmesh et al., "Development of sustainable alternative materials for the construction of green buildings using agricultural residues: a review," *Constr. Build. Mater.*, vol. 368, pp. 130457, Mar 2023, http://doi.org/10.1016/j.conbuildmat.2023.130457.

[6] H. Moayedi, B. Aghel, M. M. Abdullahi, H. Nguyen, and A. Safuan A Rashid, "Applications of rice husk ash as green and sustainable biomass," *J. Clean. Prod.*, vol. 237, pp. 117851, Nov 2019, http://doi.org/10.1016/j.jclepro.2019.117851.

[7] Z. E. N. Millogo, E. Appiah-Effah, K. Akodwaa-Boadi, A. B. Antwi, and M. N. L. Ofei-Quartey, "The synergy between pristine rice husk biomass reuse and clean energy production," *Bioresour. Technol. Rep.*, vol. 19, pp. 101179, Sep 2022, http://doi.org/10.1016/j.biteb.2022.101179.

[8] D. G. Nair, A. Fraaij, A. A. K. Klaassen, and A. P. M. Kentgens, "A structural investigation relating to the pozzolanic activity of rice husk ashes," *Cement Concr. Res.*, vol. 38, no. 6, pp. 861–869, Jun 2008, http://doi.org/10.1016/j.cemconres.2007.10.004.

[9] B. A. Tayeh, R. Alyousef, H. Alabduljabbar, and A. Alaskar, "Recycling of rice husk waste for a sustainable concrete: a critical review," *J. Clean. Prod.*, vol. 312, pp. 127734, 2021, http://doi.org/10.1016/j.jclepro.2021.127734.

[10] C. Fapohunda, B. Akinbile, and A. Shittu, "Structure and properties of mortar and concrete with rice husk ash as partial replacement of ordinary Portland cement: a review," *Int. J. Sustain. Built Environ.*, vol. 6, no. 2, pp. 675–692, Dec 2017, http://doi.org/10.1016/j.ijsbe.2017.07.004.

[11] N. S. Msinjili, W. Schmidt, A. Rogge, and H.-C. Kühne, "Rice husk ash as a sustainable supplementary cementitious material for improved concrete properties," *Afr. J. Sci. Technol. Innov. Dev.*, vol. 11, no. 4, pp. 417–425, 2019, http://doi.org/10.1080/20421338.2018.1513895.

[12] E. Marangon et al., "Mortars produced with an environmentally sustainable rice HUSK silica: rheological properties," *J. Clean. Prod.*, vol. 287, pp. 125561, Mar 2021, http://doi.org/10.1016/j.jclepro.2020.125561.

[13] M. F. Alnahhal, U. J. Alengaram, M. Z. Jumaat, F. Abutaha, M. A. Alqedra, and R. R. Nayaka, "Assessment on engineering properties and CO2 emissions of recycled aggregate concrete incorporating waste products as supplements to Portland cement," *J. Clean. Prod.*, vol. 203, pp. 822–835, Dec 2018, http://doi.org/10.1016/j.jclepro.2018.08.292.

[14] E. Ozturk, C. Ince, S. Derogar, and R. Ball, "Factors affecting the CO2 emissions, cost efficiency and eco-strength efficiency of concrete containing rice husk ash: a database study," *Constr. Build. Mater.*, vol. 326, pp. 126905, Apr 2022, http://doi.org/10.1016/j.conbuildmat.2022.126905.

[15] V. Jittin, A. Bahurudeen, and S. D. Ajinkya, "Utilisation of rice husk ash for cleaner production of different construction products," *J.*

Clean. Prod., vol. 263, pp. 121578, Aug 2020, http://doi.org/10.1016/j.jclepro.2020.121578.

[16] R. K. Sandhu and R. Siddique, "Influence of rice husk ash (RHA) on the properties of self-compacting concrete: a review," *Constr. Build. Mater.*, vol. 153, pp. 751–764, Oct 2017, http://doi.org/10.1016/j.conbuildmat.2017.07.165.

[17] T. V. Fonseca, M. A. S. Anjos, R. L. S. Ferreira, F. G. Branco, and L. Pereira, "Evaluation of self-compacting concretes produced with ternary and quaternary blends of different SCM and hydrated-lime," *Constr. Build. Mater.*, vol. 320, pp. 126235, Feb 2022, http://doi.org/10.1016/j.conbuildmat.2021.126235.

[18] H. A. A. Diniz, M. A. S. Anjos, A. K. A. Rocha, and R. L. S. Ferreira, "Effects of the use of agricultural ashes, metakaolin and hydrated-lime on the behavior of self-compacting concretes," *Constr. Build. Mater.*, vol. 319, pp. 126087, Feb 2022, http://doi.org/10.1016/j.conbuildmat.2021.126087.

[19] I. Y. Hakeem, I. S. Agwa, B. A. Tayeh, and M. H. Abd-Elrahman, "Effect of using a combination of rice husk and olive waste ashes on high-strength concrete properties," *Case Stud. Constr. Mater.*, vol. 17, e01486, Dec 2022, http://doi.org/10.1016/j.cscm.2022.e01486.

[20] M. Hamza Hasnain, U. Javed, A. Ali, and M. Saeed Zafar, "Eco-friendly utilization of rice husk ash and bagasse ash blend as partial sand replacement in self-compacting concrete," *Constr. Build. Mater.*, vol. 273, pp. 121753, Mar 2021, http://doi.org/10.1016/j.conbuildmat.2020.121753.

[21] G. Sua-iam, N. Makul, S. Cheng, and P. Sokrai, "Workability and compressive strength development of self-consolidating concrete incorporating rice husk ash and foundry sand waste: a preliminary experimental study," *Constr. Build. Mater.*, vol. 228, pp. 116813, Dec 2019, http://doi.org/10.1016/j.conbuildmat.2019.116813.

[22] N. Makul, "Combined use of untreated-waste rice husk ash and foundry sand waste in high-performance self-consolidating concrete," *Results Mater.*, vol. 1, pp. 100014, Aug 2019, http://doi.org/10.1016/j.rinma.2019.100014.

[23] V. Jittin, S. N. Minnu, and A. Bahurudeen, "Potential of sugarcane bagasse ash as supplementary cementitious material and comparison with currently used rice husk ash," *Constr. Build. Mater.*, vol. 273, pp. 121679, Mar 2021, http://doi.org/10.1016/j.conbuildmat.2020.121679.

[24] R. G. D. Molin Fo., D. A. Longhi, R. C. T. Souza, R. D. Vanderlei, P. R. Paraíso, and L. M. M. Jorge, "Study of the compressive and tensile strenghts of self-compacting concrete with sugarcane bagasse ash," *Rev. IBRACON Estrut. Mater.*, vol. 12, no. 4, pp. 874–883, 2019, http://doi.org/10.1590/s1983-41952019000400009.

[25] E. M. Raisi, J. Vaseghi Amiri, and M. R. Davoodi, "Mechanical performance of self-compacting concrete incorporating rice husk ash," *Constr. Build. Mater.*, vol. 177, pp. 148–157, Jul 2018, http://doi.org/10.1016/j.conbuildmat.2018.05.053.

[26] E. M. Raisi, J. Vaseghi Amiri, and M. R. Davoodi, "Influence of rice husk ash on the fracture characteristics and brittleness of self-compacting concrete," *Eng. Fract. Mech.*, vol. 199, pp. 595–608, Aug 2018, http://doi.org/10.1016/j.engfracmech.2018.06.025.

[27] M. Sathurshan et al., "Untreated rice husk ash incorporated high strength self-compacting concrete: properties and environmental impact assessments," *Environ. Chall.*, vol. 2, pp. 100015, Jan 2021, http://doi.org/10.1016/j.envc.2020.100015.

[28] B. Kannur and H. S. Chore, "Low-fines self-consolidating concrete using rice husk ash for road pavement: an environment-friendly and sustainable approach," *Constr. Build. Mater.*, vol. 365, pp. 130036, Feb 2023, http://doi.org/10.1016/j.conbuildmat.2022.130036.

[29] J. Safari, M. Mirzaei, H. Rooholamini, and A. Hassani, "Effect of rice husk ash and macro-synthetic fibre on the properties of self-compacting concrete," *Constr. Build. Mater.*, vol. 175, pp. 371–380, Jun 2018, http://doi.org/10.1016/j.conbuildmat.2018.04.207.

[30] F. Ameri, P. Shoaei, N. Bahrami, M. Vaezi, and T. Ozbakkaloglu, "Optimum rice husk ash content and bacterial concentration in self-compacting concrete," *Constr. Build. Mater.*, vol. 222, pp. 796–813, Oct 2019, http://doi.org/10.1016/j.conbuildmat.2019.06.190.

[31] Associação Brasileira de Normas Técnicas, *Sulphate Resistant Portland Cements*, ABNT NBR 5737, 1992.

[32] Silica Nobre. https://silcca.com.br/ (accessed Mar. 8, 2024).

[33] J. D. M. Angel, T. G. P. Vasquez, J. A. Junkes, and D. Hotza, "Characterization of ash from combustion of rice husk in a fluidized bed reactor," *Quim. Nova*, vol. 32, no. 5, p. 1110–1114, 2009, http://doi.org/10.1590/S0100-40422009000500006.

[34] L. Benassi et al., "Comparison between rice husk ash grown in different regions for stabilizing fly ash from a solid waste incinerator," *J. Environ. Manage.*, vol. 159, pp. 128–134, 2015, http://doi.org/10.1016/j.jenvman.2015.05.015.

[35] D. Silva, E. Pachla, E. Marangon, M. Tier, and A. P. Garcia, "Effects of rice husk ash and wollastonite incorporation on the physical and thermal properties of refractory ceramic composites," *Materia*, vol. 25, no. 3, e12802, Sep 2020, http://doi.org/10.1590/s1517-707620200003.1102.

[36] Associação Brasileira de Normas Técnicas, *Pozzolanic Materials – Determination of the Performance Index with Portland Cement at 28 Days*, ABNT NBR 5752, 2014.

[37] Associação Brasileira de Normas Técnicas, *Pozzolanic Materials – Determination of Calcium Hydroxide Fixed – Modified Chapelle's Method*, ABNT NBR 15895, 2010.

[38] AFNOR Association. "Standard NF P18-513". https://www.boutique.afnor.org/en-gb/standard/nf-p18513/addition-for-concrete-metakaolin-specifications-and-conformity-criteria/fa175740/39605 (accessed Sep. 14, 2022).

[39] G. C. Cordeiro, R. D. Toledo Fo., and E. M. R. Fairbairn, "Use of ultrafine rice husk ash with high-carbon content as pozzolan in

high performance concrete," *Mater. Struct.*, vol. 42, no. 7, pp. 983–992, Aug 2009, http://doi.org/10.1617/s11527-008-9437-z.

[40] N. C. Consoli, R. B. Saldanha, J. E. C. Mallmann, T. M. de Paula, and B. Z. Hoch, "Enhancement of strength of coal fly ash–carbide lime blends through chemical and mechanical activation," *Constr. Build. Mater.*, vol. 157, pp. 65–74, 2017, http://doi.org/10.1016/j.conbuildmat.2017.09.091.

[41] B. F. Tutikian and M. Pacheco, "Self-compacting concretes (SCC): comparison of methods of dosage," *Rev. IBRACON Estrut. Mater.*, vol. 5, no. 4, pp. 500–529, 2012, http://doi.org/10.1590/S1983-41952012000400006.

[42] P. C. Gomes, *Optimization and Characterization of High-Strength Selfcompacting Concrete.* Barcelona: Universitat Politécnica de Catalunya, 2002.

[43] American Society for Testing and Materials, *Standard Test Method for Bulk Density (Unit Weight) and Voids in Aggregate*, ASTM C29/C29M-07, 2009.

[44] E. Marangon, "Caracterização material e estrutural de concretos autoadensáveis reforçados com fibras de aço," Ph.D. dissertation, Univ. Fed. Rio de Janeiro, Rio de Janeiro, 2011. [Online]. Available: http://objdig.ufrj.br/60/teses/coppe_d/EderliMarangon.pdf

[45] Associação Brasileira de Normas Técnicas, *Portland Cement Concrete – Preparation, Control, Receipt and Acceptance – Procedure*, ABNT NBR 12655, 2022.

[46] Associação Brasileira de Normas Técnicas, *Self-Consolidating Concrete – Part 1: Classification, Control and Receipt in the Fresh State*, ABNT NBR 15823, 2017.

[47] EFNARC, *The European Guidelines for Self-Compacting Concrete*, 2005.

[48] Associação Brasileira de Normas Técnicas, *Concrete – Compression Test of Cylindrical Specimens*, ABNT NBR 5739, 2018.

[49] Associação Brasileira de Normas Técnicas, *Concrete and Mortar – Determination of the Tension Strength by Diametrical Compression of Cylindrical Test Specimens*, ABNT NBR 7222, 2011.

[50] Comité Euro-International du Béton, *CEB-FIP Model Code 1990*, 1993, http://doi.org/10.1680/ceb-fipmc1990.35430.

Author contributions: LEK: conceptualization, supervision, writing, formal analysis, methodology; EM: conceptualization, formal analysis, methodology, writing; JBD: data curation, formal analysis; MMC: review, writing.

Editors: Edna Possan, Daniel Cardoso.